Evidence of Elongated Polymeric Aggregates in Nafion

Laurent Rubatat,† Anne Laure Rollet,†,‡ Gérard Gebel,† and Olivier Diat*,†

Département de Recherche Fondamentale sur la Matière Condensée, SI3M, Groupe Polymères Conducteurs Ioniques, CEA-Grenoble, 17 av. des Martyrs, 38054 Grenoble Cedex 9, France; and CNRS, Centre de Recherches sur les Matériaux à haute Température, 1 D avenue de la recherche scientifique, 45071 Orléans Cédex 2, France

Received September 5, 2001; Revised Manuscript Received January 23, 2002

ABSTRACT: Small-angle X-ray and neutron-scattering techniques have been used to probe the structure of swollen Nafion membranes in the range 10−10000 Å. From analyzing the scattering data as a function of the polymer volume fraction and using a contrast variation method for the neutron experiments, we suggest a new structural model of Nafion in the hydrated state. It is based on the aggregation of the ionomer chains into elongated polymeric bundles with a diameter on the order of 40 Å and a length larger than 1000 Å, surrounded by the electrolyte solution.

Introduction

Ionomer membranes are usually depicted on an array of ionic clusters swollen by water dispersed in a continuous polymeric matrix.[1] For perfluorinated ionomer membranes, numerous articles described thermodynamical models that allow one to determine the shape of these clusters when they are hydrated and their distribution on a nanometer scale.[2−4] With different techniques including scattering, spectroscopy, and microscopy, the local ordering of these clusters as well as their sizes was intensively studied as a function of the equivalent weight, the water content, the temperature, and the nature of the ionic sites and of the counterions.[5−7] It has been shown that above 10% in water volume fraction, these clusters formed a connected network. This cluster network is described in terms of a percolation model that accounts semiquantitavely for scattering and transport data.[8−10] However, this model develops weaknesses when used to describe membranes over a wide range of swelling states. Numerous studies were performed on the dried and swollen Nafion membranes on one hand[3,4] and in solution[11,12] or in a gel state[13,14] on the other hand, and very different structural models were described without giving a coherent scheme of the swelling and dilution in such systems. Only a few studies have been performed in order to investigate the full range of structural evolution from dry membrane to solution. So far the only model attempting to rationalize the scattering data over a wide range of water content was described in ref 15. However, a structural inversion with no thermodynamical support has to be evoked to explain qualitatively this evolution between a dispersion of connected spherical ionic domains in the polymer matrix (or inverted micelles) for the low water volume fraction regime and a network of rodlike polymer aggregates for the diluted system. To confront these difficulties, we have undertaken to study Nafion-type membranes in different swelling states on a very wide range of scattering vectors. Our results reveal a scattering regime suggesting cylindrical or ribbonlike polymeric aggregates, surrounded by the ionic groups and the water molecules. This analysis allows extending the model of elongated polymer aggregates, already used for highly dilute perfluorosulfonated ionomers, to the membrane case.

* To whom correspondence should be addressed: E-mail: odiat@cea.fr.

† Groupe Polymères Conducteurs Ioniques, CEA-Grenoble.

‡ CNRS, Centre de Recherches sur les Matériaux à haute Température.

Experimental Section

We present mainly data from Nafion 117, purchased from du Pont de Nemours but the study was performed also with Nafion 115 (different thickness) and others perfluorinated ionomers (Aciplex, Dow), showing a similar behavior. Nafion 117 membrane is characterized by its equivalent weight, 1100 g/equiv, and its thickness, 175 μm, in a dry state. The standard procedures were used for the membrane preparation in term of cleaning; the membrane is soaked for 2 h in HCl 1 M and then for 2 h in NaOH 1 M. This operation is repeated twice, and then the membrane is left for 1 h in boiling deionized water. Ionic exchanges either in Li-, Cs-, or $N(CH_3)_4$-neutralized form were chosen depending on the experiment. For each case, the membrane is equilibrated in an electrolyte solution for 2 days with a renewing of the solution, at least three times a day. Then the membrane is rinsed in pure water to remove the excess of salt. The swelling from about 90% to 10% in polymer volume fraction, ϕ_p, was obtained either by using a homemade water humidity controlled cell with different salt saturated solutions or by swelling the film in a water-filled autoclave, at different temperatures. The polymer volume fraction is determined by weighing the water uptake. The value of ϕ_p is calculated using 2.1 g/cm^3 for the polymer density.

Small-angle scattering techniques are extremely suitable probes of the morphology of multiphase materials such as ionomer films, whose the structure exhibits features with length scales varying from nanometers to micron. Moreover, contrast variation, using isotopic substitutions allows to distinguish between the shape and the spatial correlation of the different polymeric domains, ion-rich or ion-poor, crystalline, or amorphous. However, to allow for reliable fitting to the model, it is important to explore the largest possible range of scattering angles. Such study is possible using high flux neutron sources and third-generation synchrotron sources having small-angle scattering spectrometers, covering a wide and comparable scattering vectors range. Small-angle neutron experiments (SANS) were performed on D22 spectrometer at the Laue-Langevin Institut (ILL, Grenoble, France). Two different configurations were used: (D_{s-d} = 2 m and λ = 6 Å) and (D_{s-d} = 17.6 m and λ = 10 Å) where D_{s-d} is the sample−detector distance and λ the incident wavelength. In this article, the scattering spectra are plotted as a function of the scattering

10.1021/ma011578b CCC: $22.00
Published on Web 04/09/2002

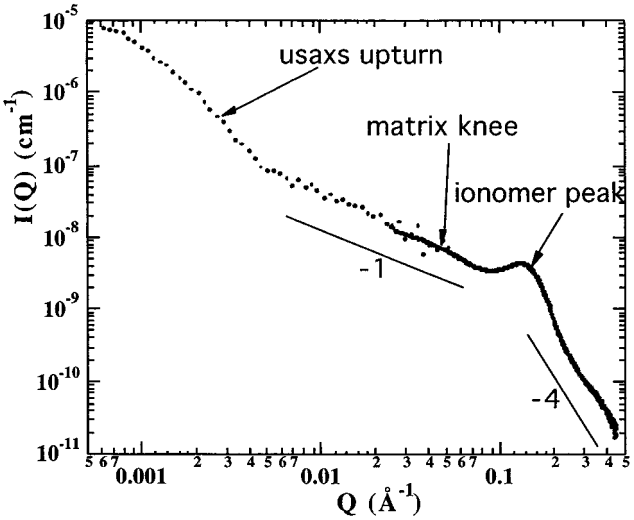

Figure 1. A log−log representation of a standard small-angle X-ray scattering curve from a swollen Nafion 117 film.

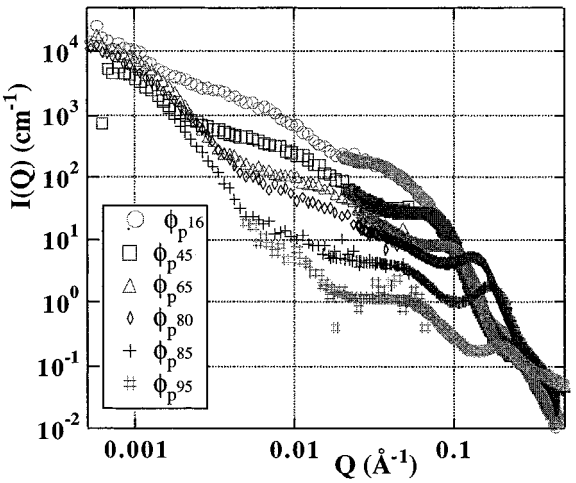

Figure 2. Radial averaged small-angle X-ray scattering data (scattering intensity vs q) for Nafion-117 membranes with different polymer volume fractions.

vector q defined as followed: $q = 4\pi/\lambda \sin(\theta/2)$ with q the scattering angle. To vary the scattering contrast between the polymer matrix, the counterions and the solvent, the sample is placed in closed quartz cell with different mixture of H_2O and D_2O. For small-angle X-ray studies (SAXS), ID02 beamline at the European Synchrotron Radiation Facility (ESRF, Grenoble, France) was quite suitable.[16] Both pinhole SAXS and ultra-SAXS camera were used in order to cover the widest range in q and to analyze the very-small-angle scattered intensity upturn with accuracy. Some SAXS experiments were also performed on the microfocus beamline, ID13, to probe the structure of the film along its thickness with a micro X-ray beam of typically 5 μm in size.[17] Standard data corrections were applied depending on the neutron or X-ray scattering methods. Although the determination of the transmission factors as well as the sample thickness for the highly swollen samples is not so accurate, the scattering spectra are given in absolute units (cm^{-1}) for comparison with other systems. For ultra-small-angle X-ray scattering (USAXS) experiments performed on ID2, no folding operations were used since crossed channel-cut analyzers were mounted for the detection scanning.[16]

Results and Discussion

As an example, we present for the first time the entire scattering curve from $q = 5 \times 10^{-4}$ up to 0.5 $Å^{-1}$ obtained by combining SAXS and USAXS experiment for a Li^+−Nafion film, swollen in water (see Figure 1). The ionomer peak is clearly visible around $q = 0.15$ $Å^{-1}$. However, a log−log representation of the data shows a strong variation of the scattering intensity over roughly six decades around this peak. From this plot we can distinguish three features. First, below 10^{-3} $Å^{-1}$, a strong upturn is observed which trends to saturate below 5×10^{-4} $Å^{-1}$. This upturn was attributed to large scale electron density inhomogeneities in the range of thousands of angstrom.[18] Second, at larger scattering angles (see Figure 1), two local maxima are distinguishable. The first one corresponds to the well-known ionomer peak. This is the main feature of the small-angle scattering curves from an ionomer film. It corresponds to the first maximum in the structure factor, which is analyzed as a local ordering between the ionic clusters. The absolute intensity and the position of this interference signal has been extensively studied as a function of the equivalent weight, the water content, the temperature, the cation exchange and the polarity of the solvent. The second one at slightly lower angle is less clearly pronounced in this swollen state and corresponds to the so-called matrix knee. Its intensity depends on the crystallinity and is usually analyzed as a supralamellar distance in the crystalline part on the polymer.[8,19] The intensity of this knee is larger because the polymer is dry and its ionic exchange capacity is low. Finally, the averaged intensity decay between 10^{-3} and 5×10^{-1} $Å^{-1}$ following a q^{-1} power law at low angles and in q^{-4} at larger angles as indicated by the straight lines in Figure 1. A q^{-1} regime between wave vectors, $2\pi/L$ and $2\pi/D$, is usually modeled as the scattering from rodlike particle with a length L and a diameter D. If we assumed a sharp interface (in scattering densities variation) for the rods, the averaged intensity decays as q^{-4} for wave vectors larger than $2\pi/D$. From Figure 1, we can estimate $D \approx 60$ Å and $L \geq 1000$ Å. This corresponds to a rather large specific surface (surface-to-volume ratio) in comparison to previous analysis on this system.[18]

However the presence of the quite large ionomer peak at the crossover between the q^{-1} and the q^{-4} scattering regimes does not allow an accurate analysis of the experimental curves over a large range of scattering vector. Actually, in the present paper, a study as a function of the polymer volume fraction was carried out in order to separate the contributions of what is highly dependent or not on the dilution.

In Figure 2 are presented different scattering curves corresponding to water-swollen Nafion films with a polymer volume fraction varying between 95 and 15%. We can clearly see that on one hand the ionomer peak as well as the matrix peak is shifted quite continuously toward the lower angles as the polymer volume fraction ϕ_p is decreasing. On the other hand, the averaged intensity decay between 10^{-3} and 5×10^{-1} $Å^{-1}$ is almost constant whatever the swelling. The q^{-1} power law variation at low angles and the q^{-4} power law at larger angles as well are still distinguishable with more or less alteration depending on the positions and intensities of both structure maxima. In fact, it is quite interesting to notice that the general shape of the scattering curves is similar whatever the membrane water swelling. This allows us to support the assumption concerning a simple dilution of the scattering entities without a strong structural reorganization of the material unlike it was suggested in ref 15.

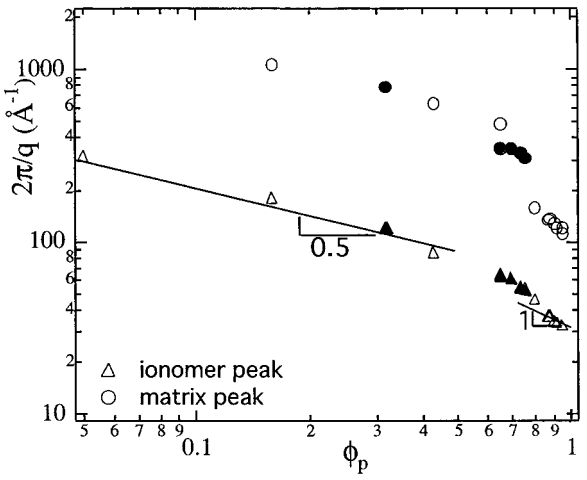

Figure 3. Inverse of the ionomer and matrix peak position as a function of the polymer volume fraction of a swollen Li^+- and Cs^+-exchanged Nafion membrane.

By plotting the position of both maxima as a function of ϕ_p or more especially the corresponding characteristic distance given by $2\pi/q^*$, two regimes can be described as has already been shown by Gebel.[15] For high ϕ_p, the swelling process described by the ionomer peak follows a power law close to ϕ^{-1} (see Figure 3).[21] For ϕ_p lower than about 60% the position of the ionomer follows a power law in $\phi^{-1/2}$ suggesting a dilution of cylindrical shaped particles. The experimental point at $\phi_p = 0.05$ is obtained from a solution of a Li^+ form of Nafion. The shaded data points correspond to swollen Nafion membrane exchanged with Cs^+ counterions. The exchange of counterions will slightly change the polymer volume fraction but not the overall structure.[7] Concerning the matrix peak position, we observed also a crossover between two regimes, around 60% in ϕ_p, which is more pronounced than that for the ionomer peak. However, the broadness of this local maximum in the scattering curves prevents an accurate determination of its q position as a function of the water content. However, an interesting point to emphasize is that the matrix peak shifts over a large q range, which is quite surprising for a crystalline distance. Moreover, the dilution laws at two different scales are correlated: one between 30 and 300 Å described by the ionomer peak and the second one between 100 and 1000 Å described by the matrix peak. It is important to remember that the swelling process of a ionomer membrane in a polar solvent is usually described as a sorption of the solvent until an equilibrium between the electrostatic forces between the solvated charges, the osmotic pressure of the counterions and the elastic deformation of the polymer chain.[22] Thus, the swelling of the perfluorinated ionomer membrane is highly temperature dependent with two different regimes, below and above the glass transition temperature of the membrane in dry state. We can probably attribute the crossover in the dilution process to the same cause since to get a sample with a polymer volume fraction below 60% we have to increase the water temperature above the T_g of the ionomer.[23]

We have of course to consider the ϕ_p power law with care, in particular for high volume fraction since the studied system is a film and not a colloidal suspension. Nevertheless, this observation can be correlated with the fact that we consider a 1D aggregation of the polymer chains. However, the difference between the swelling of the film and the dilution of a suspension might be revealed in analyzing the change in the matrix peak or even the ultra-small-angle upturn. But up to now, no clear model can be established at this mesoscopic scale.

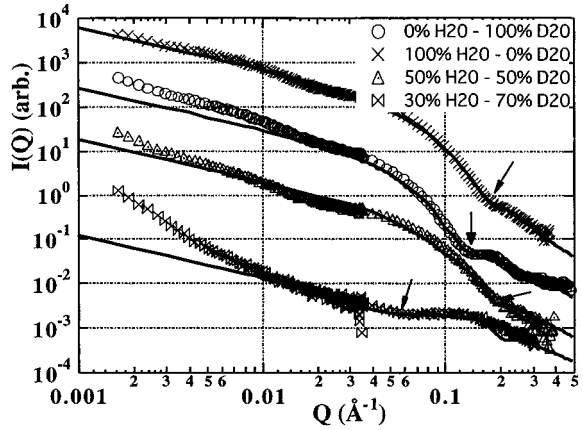

Figure 4. Contrast variation data: SANS curves for a swollen $N(CH_3)_4$−Nafion membrane with $\phi_p = 16\%$ and four different H_2O/D_2O ratios. Solid curves correspond to the form factor simulation of shell cylinders taking into account the contrast variation from the solvent. The four arrows indicate the position of the first minimum for each curve, a minimum related to the counterions shell interferences.

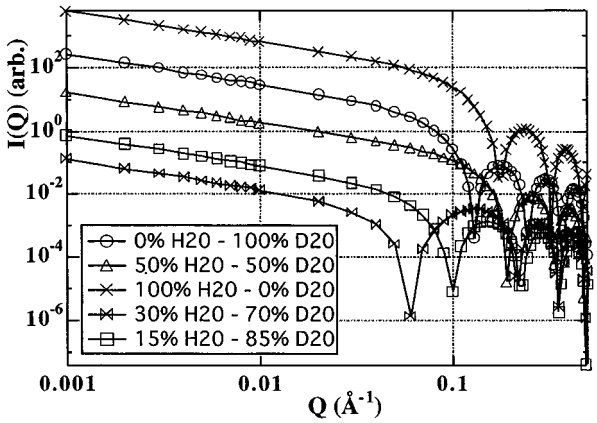

Figure 5. Simulated SANS curves (from eq 2) for a swollen $N(CH_3)_4$−Nafion membrane with $\phi_p = 16\%$ and five different H_2O/D_2O ratios indicated in the legend. They correspond to the form-factor simulation of shell cylinders taking in account the contrast variation from the solvent. The position of the first minimum is very sensitive to the contrast variation since the counterion shell is highly protonated.

To analyze more precisely the part of the scattering curve, which is practically not dependent on the swelling process, the contrast variation method in small-angle neutron scattering appears to be very suitable. In Figure 4, we present four sets of data corresponding to the scattering curves of a water-swollen $N(CH_3)_4$−Nafion membrane with $\phi_p = 16\%$ for different H_2O/D_2O ratio. This type of experiment was carried out also for higher polymer volume fractions (see such an example in Figure 6); however for $\phi_p = 16\%$, the ionomer as well as the matrix peak is not so well pronounced and are shifted to the lowest scattering angle. Thus, this latter case appears to be more convincing to support our proposal.

In this graph, we can observe that the shapes of the scattering curves are significantly different, as a function of the H_2O/D_2O ratio. Actually, this continuous variation from fully protonated to fully deuterated water allows changing the contrast between the scattering

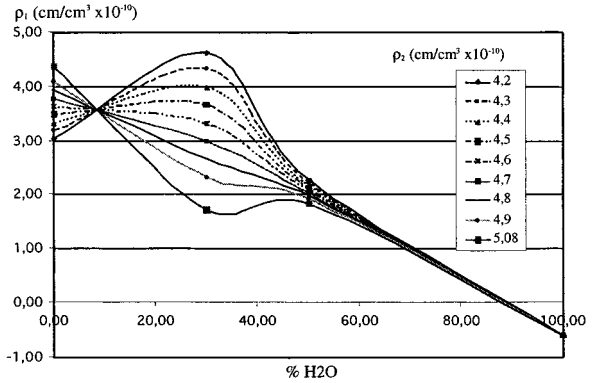

Figure 6. Plot of ρ_1, the counterion shell scattering length density (SLD), as a function of the solvent SLD ρ_0 and for different polymeric core SLDs (between 4.21 in complete amorphous state and 5.08×10^{10} cm/cm^3 in the fully crystalline state) and as determined from the fit parameter $(\rho_2 - \rho_1)/(\rho_1 - \rho_0)$.

aggregates and the solvent. If we consider only a biphasic structure *seen* by the neutrons—the polymer and the solvent with the counterions—the intensity of the whole scattering curves should scale simply as the square of the scattering densities difference and this is not the case for the $N(CH_3)_4^+$-exchanged Nafion membrane.

Now, if we describe the interface between the polymeric parts and the water domains by a condensed layer of the solvated counterions, using a two-step model for the scattering length density (SLD), we can really analyze these scattering curves as the signature of the interferences between the three domains.[20] Moreover, the shift of local minima as a function of the H_2O/D_2O ratio—indicated by arrows in Figure 4—discriminates with no ambiguity between a cluster of water in a polymeric matrix or a cluster of polymer surrounding with the solvent.[20] For this latter case, only an entanglement of elongated aggregates can be considered in order to match the film properties. Thus, to analyze the scattering curves, we have to define the form factor $F(\vec{q})$ for a cylinder of axial semilength L and cross-sectional radius R, which is given by

$$F(\vec{q}) = F(q,\gamma,L,R) = \rho_0 V \frac{\sin(qL\cos(\gamma))}{qL\cos(\gamma)} \frac{2J_1(qR\sin(\gamma))}{qR\sin(\gamma)} \quad (1)$$

with γ the angle between $\vec{q}$ and the cylinder axis and V the volume of the particle. ρ_0 is the difference in scattering length density (SLD) between the particle and the solvent, and $J_1(x)$ is the first-order Bessel function of the first kind. In our case, if we consider the form factor of a shell-cylinder with a polymeric core characterized by a SLD ρ_2 surrounded with the condensed counterions shell (ρ_1) and the solvent (ρ_0) and taking in account the average over all particle orientations, then the scattered intensity, with the assumption that the interaction between the objects are negligible, can be written as

$$I(\vec{q}) = K\langle|F(\vec{q},L,R,e)|^2\rangle_{\vec{q}} = K\int_0^{\pi}\left[F(q,\gamma,L,R+e) + \frac{\rho_2-\rho_1}{\rho_1-\rho_0}\frac{V(R)}{V(R+e)}F(q,\gamma,L,R)\right]^2 \sin(\gamma)\,dr \quad (2)$$

with R the core radius, e the thickness of the counterion condensed layer, and $V(r)$ the volume of the cylinder with a radius r. The constant K is only a function of the radii, the corresponding SLD ρ_i, and experimental factors.

In Figure 5, we have plotted $I(\vec{q})$ for $2L > 1000$ Å, the polymeric cross-section $R = 22$ Å, the counterion shell thickness $e = 5$ Å and different contrast parameters $(\rho_2 - \rho_1)/(\rho_1 - \rho_0)$. The shift of the first minimum is sensitive to the contrast variation and depends strongly on the SLD of the inner part of the scattering object, that means the polymer SLD in our model instead of the solvent SLD for the case of "inverted micelles".[8]

To analyze the experimental scattering curves, since the oscillations in the Porod region are quite smooth,[23] we have taken into account a polydispersity of 20% with a Gaussian distribution function for the core radius. We can clearly see in Figure 4 (full curves) that the adjustment using our model is quite good and the assumption of a rodlike aggregate as a scattering entity allows one to analyze the data with few parameters. For a set of data corresponding to the same volume fraction but with different contrasts, once the inner radius, the counterion shell thickness, and the rod length are fixed, only a contrast parameter $(\rho_2 - \rho_1)/(\rho_1 - \rho_0)$ has to be adjusted. It corresponds to the ratio of the scattering density difference between the polymeric inner part and the hydrated counterion shell with the scattering density difference between the hydrated counterion shell and the solvent. From the adjustment shown in Figure 4, this ratio is equal to -100, -3, -1.33, and -0.5 for 100, 50, 30, and 0% of H_2O in the mixture $H_2O + D_2O$, respectively. Since the solvent SLD ranges from -0.56×10^{10} cm/cm^3 in pure H_2O to 6.39×10^{10} cm/cm^3 in pure D_2O and the polymeric core SLD ρ_2 has a value between 4.21 (in complete amorphous state) and 5.08×10^{10} cm/cm^3 (in the fully crystalline state), we can draw the graph in Figure 6. It corresponds to the variation of the interfacial SLD as a function of ρ_2. So, assuming that ρ_1 for the solvated protonated counterions should be a monotonic function of the ratio between H_2O and D_2O, then we determine a polymer core SLD around 4.7×10^{10} cm/cm^3. This value is quite similar to what it has been obtained from contrast variation analysis in Nafion H^+ alcohol solution in ref 11.

For more concentrated membrane (see Figure 6), the scattering profiles depending on the contrast variation is similar to those displayed in Figure 4 for three different H_2O/D_2O ratios. Unlike the previous case, it is obviously more difficult to analyze this scattering curve due to the presence of the correlation peaks. The respective structural interferences with their maxima (and minima) disturb strongly the averaged scattering decrease, which is nevertheless qualitatively comparable with those of highly swollen samples. Moreover, we can observe, depending on the contrast, that a minimum around 10^{-2} Å^{-1} in the scattering curve is shifting in the q position as is observed for the highly swollen sample and the ionomer peak may vanished when the solvent is fully deuterated. However, since the structure factor cannot be dissociated from the form factor of the scattering objects—the geometry of these aggregates is not centrosymmetric and the polymer concentration is high—we can only emphasize some relative intensity variations at different q vectors. For example, it is important to point out that we observe an increase of the intensity level and a shift to the larger scattering

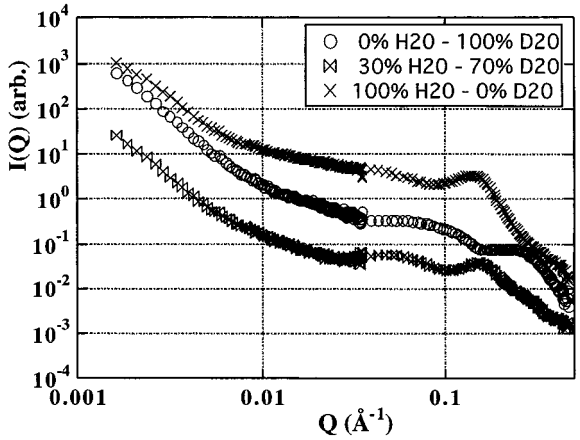

Figure 7. Contrast variation data: SANS curves for a swollen $N(CH_3)_4$−Nafion membrane with $\phi_p = 80\%$ and three different H_2O/D_2O ratios.

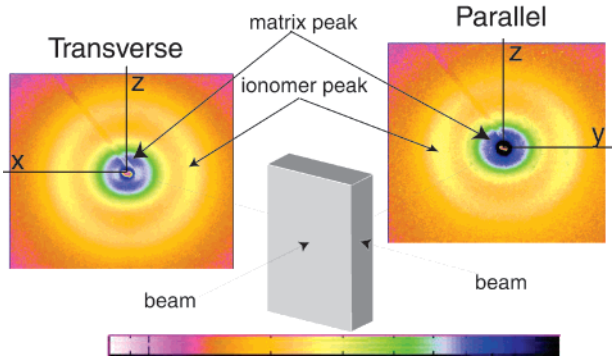

Figure 8. 2D- X-ray scattering profiles obtained in a transverse configuration (the microbeam illuminates the membrane along its thickness) and in parallel configuration (the microbeam illuminates the membrane perpendicular to its surface). The ionomer and the matrix rings are indicated with arrows. The intensity log scale is displayed below.

angles of the smooth oscillations in the Porod region. Relative to our model, this can be interpreted as an apparent decrease of the core radius from typically 22 Å in the hyperswollen state to about 14 Å in the dry state. This can still be understood as a temperature effect, allowing higher chain mobility and an apparent swelling of the aggregates themselves with the solvatation of the sulfonated ionic groups. Of course, these values are extracted from a rather crude model for a complex polymeric system. Nevertheless, it allows one to extract two characteristic lengths, one for the transversal size or apparent diameter of the scattering entities and the second for its axial length, larger than 1000 Å.

Finally, we can consider the ionomer peak as a signature of the mean distance between the polymeric aggregates, its position variation in $\phi^{-1/2}$ below $\phi_p = 60\%$ being in quite good agreement with a dilution law of apparent rodlike particles. This assumption is not sufficient to explain the change in the dilution process around $\phi = 60\%$ between $\phi^{-1/2}$ and roughly ϕ^{-1}, except if we consider that the aggregates are more ribbonlike instead to be rodlike. This type of aggregate has been already suggested in ref 23. Then, from the analysis of the Porod region for which the absolute intensity is proportional to the surface of the scattering object over the scattering volume ratio, we can determine a polymeric thickness and a width close to 20 and 80 Å respectively, for ribbonlike aggregates. This is coherent with the dilution process crossover observed in Figure 2 below 100 Å. As a matter of fact, for a distance between the aggregates larger than 80 Å, the orientation distribution of the particles around the long axis becomes isotropic and they can be considered as cylinders. On the other hand, for high polymer volume fraction, the aggregates are packed together in domains face to face, and the dilution process is certainly more complex. Nevertheless, we can consider at first order that the dilution process is similar to those of a lamellar structure for which the dilution law is characterized with an exponent of 1.[21]

Concerning the matrix peak which has been shown in other articles to be strongly correlated with the long period of the crystallinity, a microSAXS experiment on H^+ Nafion membrane has been performed in two orthogonal configurations (see Figure 8). It permitted us to emphasize a structural anisotropy, which can be revealed also with optical observations between crossed polarizers. This type of experiment does not allow to evidence if this anisotropy is induced by the industrial processing or comes from an intrinsic anisotropy in the nanoaggregation as rodlike particles, not randomly distributed, but it indicates that the scattering contribution from the ionomer and the matrix peak are distinct and even orthogonal. We can clearly see in Figure 8 that the intensity of the ionomer peak is more intense along the *x* and *y* directions when the matrix peak intensity is higher along the *z* direction, parallel to the casting process. These observations will allow us in a next step to analyze as a function of the scattering vector direction the small-angle scattering bump related to the weak crystallinity of the material and the form factor of the polymeric aggregates, for very-well-oriented samples.

Finally, the high angular resolution of USAXS technique allows to analyze accurately the very-small-angle scattering upturn of the spectra, usually attributed to large scale inhomogeneities. Assuming an exponential form for the density correlation function[24] (Debye−Bueche model) which fits quite well the intensity variation over 1 decade in *q* values (see Figure 9), leads to the identification of a characteristic size on the order of 800−1000 Å. This value depends slightly on the perfluorinated ionomers studied (Aciplex, Dow) and can be only determined with accuracy when the membrane are partially swollen. As a matter of fact, the Figure 4 shows that this upturn is less pronounced for highly swollen samples or for practically dried samples for which the contrast at large scale is certainly quite weak. However, to go further in the scattering data analysis, and especially at the micrometer scale, it would be interesting to consider that the bundles or the packing of elongated polymeric aggregates in larger domains would give rise to this strong scattering upturn.

Conclusion

From the scattering point of view, it is clear that the structure of Nafion membrane is quite complex and presents some density variation at different scales from nanometers up to micrometers. Since the scattering data reflects the Fourier transform of the real structure, we cannot consider only the signal around the ionomer peak but over a larger scattering range. From the contrast variation method combined with the SANS technique, the structure between 10 and 1000 Å of the Nafion can be described in term of elongated polymeric

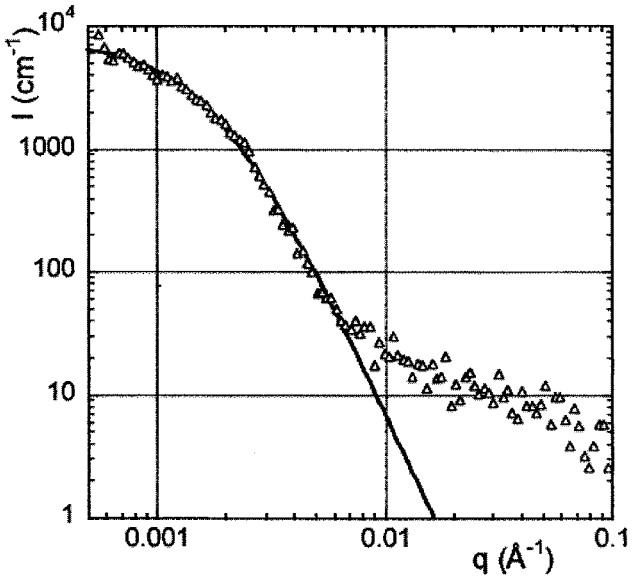

Figure 9. Ultra-small-angle scattering intensity profile of Li^+ Nafion 115 membrane vs q and the corresponding adjustment intensity (solid curve) using a Debye−Bueche density correlation function (with a characteristic length of 750 Å).

aggregates connected at larger scale to form a film with good mechanical properties. The water swelling process allows to separate these aggregates following two different regimes depending on the hydration: a lamellar dilution at low water content and a 2D swelling for polymer volume fraction higher than 60%. Our crude model in term of more or less elongated polymeric aggregate is coherent with the evolution of the structure as a function of the water content until the solution. Finally, a deeper study on the crystallinity dependence for the shift of the so-called matrix peak as well as orientation studies is highly desirable in order to really point out the role of the polymer backbone arrangement in the aggregates, the orientation distribution of these aggregates, and the long-range correlation observed at the submicrometer scale.

Acknowledgment. The authors are grateful to the Institut Laue Langevin for providing beamtime and I. Grillo as local contact for her help in achievement of SANS experiments and the European Synchrotron Radiation Facility (SC729) with the ID2 team for SAXS experiments as well.

References and Notes

(1) Eisenberg, A. *Macromolecules* **1970**, *3*, 147.
(2) Eisenberg, A.; Yeager, H. L. *Perfluorinated Ionomer Membranes*; ACS Symposium Series 180; American Chemical Society: Washington, DC, 1982.
(3) Pineri, M.; Eisenberg, A. *Structure and Properties of Ionomers*; D. Reidel Publishing Co.: Dordrecht, The Netherlands, 1987.
(4) Schlick, S. *Ionomers: Characterization, Theory and Applications*; CRC Press: Boca Raton, FL, 1996.
(5) Register, R. A.; Cooper, S. L. *Macromolecules* **1990**, *23*, 318.
(6) Elliot, J. A.; Hanna, S.; Elliot, A. M. S.; Cooley, G. E. *Macromolecules* **2000**, *33*, 4161.
(7) Rollet, A.-L.; Gebel, G.; Simonin, J.-P.; Turq, P. *J. Polym. Sci., Part B: Polym. Phys.* **2001**, *39*, 548.
(8) Gierke, T. D.; Munn, G. E.; Wilson, F. C. *J. Polym. Sci., Polym. Phys. Ed.* **1981**, 19, 1687.
(9) Kreuer, K. D. *J. Membr. Sci.* **2001**, *185*, 29.
(10) Wodski, R.; Narebska, A.; Kwas, W. *J. Appl. Polym. Sci.* **1985**, *30*, 769.
(11) Loppinet, B.; Gebel, G.; Williams, C. E. *J. Phys. Chem. B* **1997**, *101*, 1884.
(12) Gebel, G.; Dubin, P.; Bock, J.; Davies, R.; Shulz, D. N.; Thies, C.; Springer-Verlag: Heidelberg, Germany, 1994.
(13) Cirkel, P. A.; Okada, T.; Kinugasa, S. *Macromolecules* **1999**, *32*, 531.
(14) Cirkel, P. A.; Okada, T. *Macromolecules* **2000**, *33*, 4921.
(15) Gebel, G. *Polymer* **2000**, 41, 5829.
(16) Narayanan, T.; Diat, O.; Bösecke, P. *Nucl. Instrum. Methods Phys. Res. A* **2001**, *467*, 1005.
(17) Riekel, C.; Burghammer, M.; Müller, M. *J. Appl. Crystallogr.* **2000**, *33*, 421.
(18) Gebel, G.; Lambard, J. *Macromolecules* **1997**, *30*, 7914.
(19) Fujimura, M.; Hashimoto, T.; Kawai, H. *Macromolecules* **1981**, *14*, 1309.
(20) Rollet, A.-L.; Diat, O.; Gebel, G. *J. Phys. Chem. B*, in press.
(21) Litt, M. H. *Polym. Prepr. (Am. Chem. Soc., Div. Polym. Chem.)* **1997**, *38*, 80.
(22) The minimization of the interfacial energy between the hydrophobic part of the polymer and the solvent has to be also taken in hand.
(23) Chomakova-Haefke, M.; Nyffenegger, R.; Schmidt, E. *Appl. Phys. A: Mater. Sci. Process.* **1994**, *59*, 151.
(24) Debye, P.; Anderson, H. R.; Brumberger, H. *J. Appl. Phys.* **1957**, *28*, 679.

MA011578B